

Pollutant Transport and Mixing Zone Simulation of Sediment Density Currents

R. L. Doneker, M.ASCE¹; J. D. Nash²; and G. H. Jirka, F.ASCE³

Abstract: Prediction of water column concentrations of suspended sediment is often necessary for environmental impact assessment of point source industrial discharges. For example, in “flow lane” or “open water” disposal, suction dredges discharge large volumes of suspended sediment into shallow water disposal locations. A sediment density current mixing model is presented here as part of the *D-CORMIX* expert system for hydrodynamic simulation of mixing zone behavior. This density current model extends the *CORMIX* decision support system to simulate continuous negatively buoyant discharges with or without suspended sediment loads on a sloping bottom with loss of suspended particles by sedimentation. Sedimentation is modeled using Stokes settling for five particle size classes. Density current width and depth, trajectory, total solids, tracer concentration, dilution, and particle size concentration are predicted. In addition, location and widths of sediment deposits, accretion rates, including particle size fractions within the spoils deposit, are predicted. The model results are in good overall agreement with available field and laboratory data.

DOI: 10.1061/(ASCE)0733-9429(2004)130:4(349)

CE Database subject headings: Pollutants; Density currents; Water pollution; Environmental quality regulations; Waste disposals; Dredge spoils; Transport phenomena.

Introduction

Information on the mixing behavior of suspended sediment plumes is often desired for water quality management and environmental impact prediction. Such turbidity current plumes can result from sources such as pipeline dredging operations, oil and gas drilling, mine tailings disposal, or other industrial processes (Ellis et al. 1995; Neves and Fernando 1995; Meinhold et al. 1996; Ruffin 1998; Black and Parry 1999; Burns et al. 1999; Mulder and Alexander 2001). Sediment density currents can also arise from natural processes such as tributary inflows to reservoirs, lahars, and debris flows (Akiyama and Stefan 1984; Alavian 1986; Chikita and Okumura 1990; Alavian et al. 1992; Fan and Morris 1992; McLeod et al. 1999; Mulder and Alexander 2001). The resulting plumes of suspended sediment may travel downslope as density currents while being advected by an ambient velocity field. Material suspended within the plume affects water quality within the water column, while particle settling from the plume forms deposits that have benthic impacts (Stow and Bowen 1980; Stacey and Bowen 1988; Garcia 1994). As a gravity driven flow, sediment density current trajectory and mixing is strongly dependent on local bathymetry, bottom slope, and ambient den-

sity structure (Fietz and Wood 1967; Parker et al. 1986; Garcia 1993; Sparks et al. 1993). Monaghan et al. (1999) give numerical results and experimental data for density currents on with varying ramp angle, however, the flows are laterally confined. Hallworth et al. (1998) report on laboratory experiments on pulsed injections creating density currents in laterally bounded laboratory flume. Lee and Yu (1977) present a laboratory study with clay in a flume. Garcia and Parker (1991) performed experiments on gravity currents driven by poorly sorted sediments in a laboratory flume. However, these experiments are two-dimensionally bounded and do not consider lateral spreading of the density current flow.

Regulatory management of natural waters often allows that point source discharges be evaluated not by “end of pipe” concentration standards but in a way that allows for the initial dilution of the discharge within a mixing zone. This approach recognizes the natural assimilative capacity of a water body to treat pollutants in an economically efficient manner. This has led to the concept of an “allocated impact zone” or “regulatory mixing zone” (RMZ) around the discharge point. Fig. 1 illustrates the RMZ, and in case the discharge contains toxic substances, a more restrictive region within the RMZ called the toxic dilution zone (TDZ) for toxic discharges. Within the RMZ and TDZ numeric water quality criteria may be exceeded as long as the water body as a whole is not impaired. Regulations concerning the size and shape of the mixing zone vary widely depending upon the regulatory authority. Channel bottoms or benthic areas are ecologically and commercially important (e.g., as fish spawning areas or oyster beds) and are often the most sensitive to the effects of point source discharges.

D-CORMIX is a near-field and far-field mixing zone model developed for water quality assessment for negatively buoyant (dense) continuous source discharges with suspended sediment loads. It extends the *CORMIX* expert system for mixing zone analysis to simulate discharges with suspended sediment (Doneker and Jirka 1990). While the system was developed pri-

¹Assistant Research Professor, Portland State Univ., Dept. of Civil and Environmental Engineering, PO Box 751, Portland, OR 97207.

²Assistant Professor, Physical Oceanography, College of Oceanic and Atmospheric Sciences, 104 Oceanic Administration Building, Oregon State Univ., Corvallis, OR 97331.

³Professor and Director, Institute for Hydromechanics, Univ. of Karlsruhe, Karlsruhe, D-76131, Germany.

Note. Discussion open until September 1, 2004. Separate discussions must be submitted for individual papers. To extend the closing date by one month, a written request must be filed with the ASCE Managing Editor. The manuscript for this paper was submitted for review and possible publication on November 16, 2001; approved on April 29, 2003. This paper is part of the *Journal of Hydraulic Engineering*, Vol. 130, No. 4, April 1, 2004. ©ASCE, ISSN 0733-9429/2004/4-349–359/\$18.00.

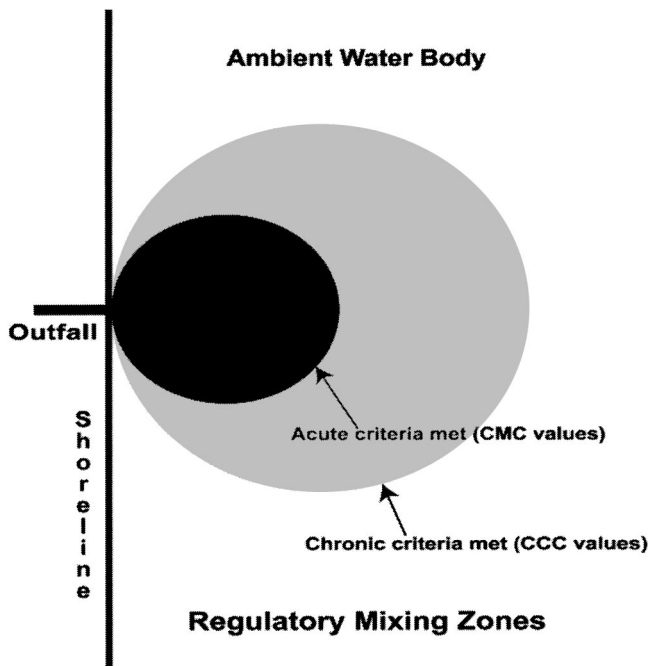
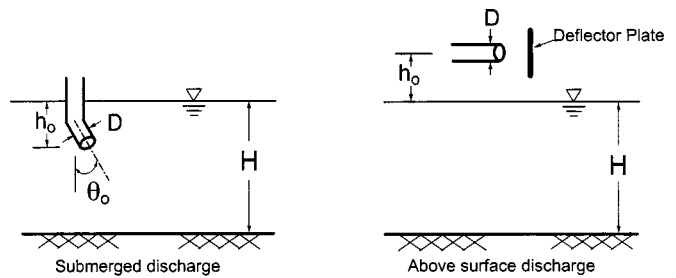


Fig. 1. Regulatory mixing zones (RMZ), defined by chronic criteria, can be located in the near-field or far-field of a discharge. Toxic dilution zones (TDZ), defined by acute criteria, almost always occur in the near-field. Adapted from: *Technical support document for water quality-based toxics control, USEPA/505/2-90-001*.

marily for dredge discharge sources, it can model density current plumes that arise from storm water discharge or desalination concentrate disposal. The model focus is on assessment of water quality within the water column, with emphasis on the resulting suspended sediment density current. However, characteristics and accretion rate of deposited sediment are also predicted. As a basic water quality assessment and sediment deposit screening tool, the model does not predict dynamic bottom scour, the affect of changing bathymetric topography due to sediment deposition on plume mechanics, or the possibility of reentrainment of previously deposited material into the suspended sediment density current plume.

D-CORMIX System Description

The system uses the DOS command prompt user-interface as *CORMIX* (Jirka et al. 1996) to input data. It follows a similar classification scheme for submerged discharges as *CORMIX1* (Doneker and Jirka 1990) and for surface discharges as *CORMIX3* (Jones et al. 1996) to determine the near field flow structure. This approach is based upon a classification scheme that determines the flow regimes that are important to a given discharge/ambient combination, and applies the appropriate jet-integral or length-scale model appropriate to each flow regime. Central to the methodology is the ability to predict dynamic boundary interactions of dense jets and plumes. Boundary interactions include near-field attachments, jet mixing over the full depth in shallow water, plunging effects, internal trapping, and three-dimensional density current behavior on either a flat bottom, inclined bottom, or trapped density level (Simpson and Britter 1979; Akiyama and Stefan 1984; Alavian 1986; Garcia 1993;



Discharge Condition Options

1. Submerged pipe Diameter D with or without deflector plate normal to discharge
Restrictions: $D/2 (\sin \theta_0) \leq H/2$, $-90^\circ \leq \theta_0 \leq 0^\circ$
2. Above surface pipeline disposal
 - a) Horizontal near-surface with or without deflector plate
 - b) Upward sprayed discharge with or without deflector plate
3. Shoreline surface negatively buoyant discharge (not shown)

Fig. 2. D-CORMIX discharge conditions assumptions

Sparks et al. 1993; Mulder and Alexander 2001). Particle settling is accounted for once bottom contact has occurred.

Several different discharge configurations are considered including submerged, surface, and above surface discharges. Fig. 2 shows typical discharge configurations considered by *D-CORMIX*. Above surface discharges can either be sprayed (1) over a large area, (2) sprayed in a single jet, or (3) sprayed onto a deflector plate, techniques which are sometimes used to spread material during pipeline dredge material disposal. Below surface jet discharges are restricted to the upper half of the water column. Shoreline discharges occur at the surface of the ambient water body, from a pipe or discharge canal.

Five sediment class sizes can be considered (large chunky solids, sand, coarse silt, fine silt, and clay) and sedimentation is modeled using Stokes settling. The model can simulate hindered Stokes settling as an option, but this process was not simulated for the initial model validation presented here. The sediment size classes and settling velocities are shown in Table 1. Chunks are assumed to deposit on the bottom immediately after discharge, while the other particle size fractions are available for transport within the density current.

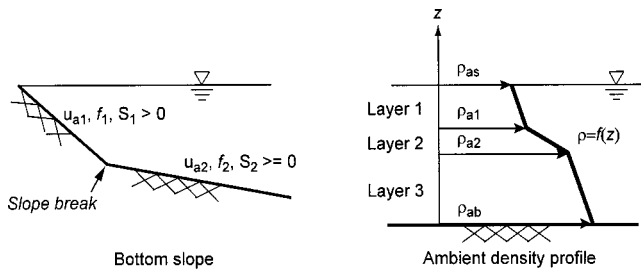
In addition, a conservative or nonconservative tracer (pollutant) may be issued in the discharge. A nonconservative pollutant can be assigned a first order decay or growth. Of course, the model can also be run without any sediment present in the discharge flow.

As shown in Fig. 3, the ambient water body may have either one or two zones (near-shore and off-shore), where different ambient velocities u_a , bottom slopes S , and Darcy friction factors f may be entered. The offshore slope S_2 may be either flat or in-

Table 1. Particle Size Class Distributions

Sediment size class	Particle size (μm)	Settling velocity (mm/s)
Chunks ^a	N/A	N/A
Sand	>62	320
Coarse silt	16–62	6.28
Fine silt	3.3–16	0.394
Clay	<3.3	0.0134

^aLarge nonsuspended solids and stones.



Ambient Condition Options

1. Uniform channel in downstream direction
2. Uniform ambient current field $u_{a1} = \text{constant}_1$; $u_{a2} = \text{constant}_2$
3. Positive near-shore slope S_1 with break to S_2
4. Bounded laterally on one side only in the near-field
5. Up to 3 layers of density stratification with arbitrary stable profile

Fig. 3. *D-CORMIX* ambient conditions assumptions

clined, while the near-slope S_1 must have some inclination. Ambient stratification, also shown in Fig. 3, is described by a surface density value, and up to three density values (other than the surface) that are known at different submergence levels below the water surface. A piecewise linear stratification is assumed to exist between these levels.

Hydrodynamic Simulation and Flow Classification

Mixing zone processes are controlled by the interplay of discharge and ambient conditions. As the discharge plume travels away from the source, the flow will interact with the ambient boundaries, current, and density profile. The *CORMIX* methodology emphasizes the role of these boundary interactions on mixing processes (Doneker and Jirka 1990). Vertical boundary interaction occurs when the flow contacts the water surface, channel bottom, or forms an internal terminal layer in a density-stratified ambient environment. Boundary interaction can define the transition from near-field to far-field mixing. Near-field mixing processes are those for which the initial momentum, buoyancy, and geometric orientation of the discharge has the predominant effect on flow behavior. Far-field mixing processes are largely controlled by ambient conditions. Fig. 4 shows mixing processes representative of a typical dredge discharge scenario: near-field buoyant jet mixing, bottom boundary interaction with upstream density current intrusion, and a far-field with lateral density current spreading followed by passive ambient diffusion. In the general case, the density current trajectory is due to two force mechanisms, the gravitational (buoyancy force) and the crossflow (entrainment and momentum transfer and drag force).

Two limiting conditions of the general case are: (1) No ambient crossflow: only gravitational flow, the density current proceeds straight down slope, and (2) No offshore slope (flat bottom): ambient crossflow controls trajectory and mixing, the density current will proceed parallel to the shoreline in the direction of the ambient flow.

The *CORMIX* flow classification uses length scales to determine the discharge/environment interaction and the flow processes that control initial near-field mixing and transition to far-field plume behavior (Jirka and Doneker 1991). The *CORMIX* classification scheme and modeling approach has undergone extensive validation by the authors and by numerous independent

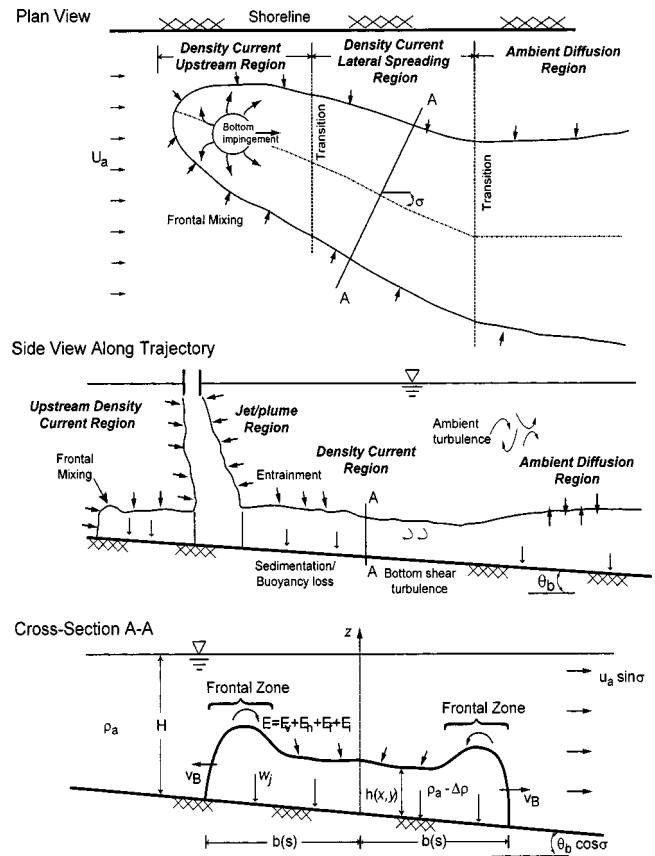


Fig. 4. Submerged negatively buoyant single port discharge into a flowing unstratified receiving water on a sloping bottom. Near-field buoyant jet mixing is terminated by boundary interaction on the channel bottom. Boundary interaction includes a stable upstream density current intrusion. In the far-field, density current mixing on the bottom slope is followed by a transition to passive diffusion.

studies (Doneker and Jirka 1990; Akar and Jirka 1991a,b; Doneker and Jirka 1991; Jirka and Akar 1991; Jirka and Doneker 1991; Akar and Jirka 1994; Tsanis et al. 1994; Akar and Jirka 1995; Nash and Jirka 1995; Gawad et al. 1996; Jones et al. 1996; Mendez Diaz and Jirka 1996; Nash and Jirka 1996; Valeo et al. 1996; Valeo and Tsanis 1996; Davies et al. 1997; Doneker and Jirka 1997, 1999). The classification system is used to identify the appropriate series of regional computational submodels employed to simulate the entire mixing process. Fig. 5 shows an example of the flow classification system of *D-CORMIX* for single port submerged discharges along with representative sketches of resulting plumes. In general, *D-CORMIX* uses a classification scheme that has been vertically inverted from the *CORMIX* flow classifications (Akar and Jirka 1991a; Jirka and Doneker 1991; Jones et al. 1996). For example, whereas *CORMIX1* is primarily concerned with buoyant discharges near the bottom, *D-CORMIX* assumes a negatively buoyant discharge near the water surface. Therefore behavior of plumes simulated by *D-CORMIX* would be represented by "mirror images" of the sketches of the standard *CORMIX* flow classifications, with the water surface replaced by the ambient bottom and vice versa; i.e., with plumes sinking to the bottom rather than rising to the surface.

Within *D-CORMIX*, the DS classes are the negatively buoyant counterparts of the *CORMIX1* classes and represent flows where stratification is important in the near field and trapping of the density current will occur within a stratified layer above the bot-

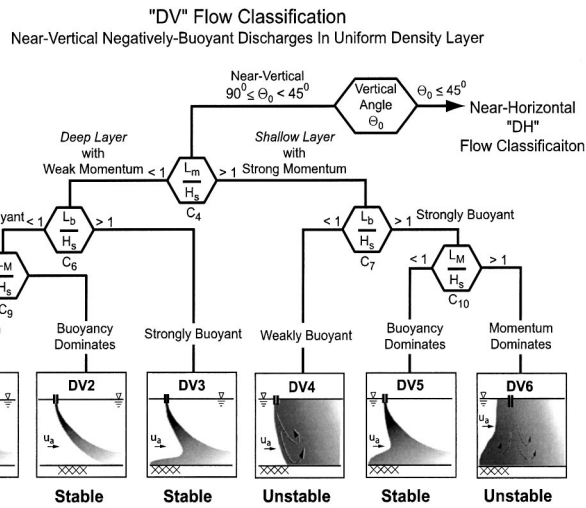


Fig. 5. *D-CORMIX* flow classification for single port discharge in a uniform density layer. The complete *D-CORMIX* classification scheme contains about 50 generic flow classes. Hydrodynamic classification ensures that the appropriate simulation model can be safely and reliably applied. For example, jet-integral modeling techniques can be used to simulate stable near-field mixing but do not apply to the unstable flow classes, where alternative length scale models can be used.

tom (Doneker and Jirka 1990). The DV and DH classes are inverted from *CORMIX1*'s V and H classes and represent flows issued near vertically (DV) or near horizontally (DH) which do not trap within the density stratification (Doneker and Jirka 1990). Thus two-dimensional flows may also be predicted where the ambient is considered shallow (e.g., the DH4, 5 and DV4–6 flow classes). In addition, many of the above flows may exhibit dynamic attachment to the water surface; these flows are further classified as attached cases D(...)A-classes, which are inverted *CORMIX1* A-classes (Doneker and Jirka 1990). Two classes, DFJ1 and DFJ3, are used to characterize negatively buoyant flows issued from the shoreline. These are similar to the *CORMIX3* system and represent the cases of free jets in deep and shallow receiving water, respectively (Jones et al. 1996).

After vertical boundary interaction and associated near-field mixing, far-field mixing will occur within a density current before the transition to passive diffusion. Density currents are gravity-driven flows that typically collapse vertically while spreading laterally. Thus density current trajectory and mixing will be affected by both ambient crossflow and bottom slope. A sediment-laden density current loses buoyancy by particle settling. Entrainment increases the volume flux and increases along the frontal head region and lateral boundaries. *D-CORMIX* allows for suspended particle sedimentation after initial mixing when the plume has contacted the bottom or has formed a terminal level in a density stratified ambient.

The computational modules used in *D-CORMIX* are similar to those used in *CORMIX1* (Doneker and Jirka 1990) and *CORMIX3* (Jones et al. 1996) with a number of modifications and additions. The simulation modules 310–362 (used for positively buoyant spreading at the surface in *CORMIX3*) have been modified so that they represent negatively buoyant density currents with sedimentation and bottom friction. In particular, MOD310 of *D-CORMIX* predicts density current behavior on an inclined plane using an integral model approach as presented in the next section. Table 2 shows abridged output from the simulation model and contains

details from the sediment density current MOD310. Table 2 also shows the predicted sediment mass flux remaining in the plume by particle size fraction as a percentage of the source sediment mass flux. The bottom sediment accretion rate and particle size distribution at downstream distances can be calculated based upon assumption of sediment discharge source duration.

Governing Equations for Bottom Density Current Model

The governing integral equations of a steady-state sediment depositing density current on an inclined plane are summarized below (Nash and Jirka 1995). The approach includes stepwise-continuous ambient density stratification, crossflow velocity, and bottom inclination. Flow on a sloping bottom with bottom detachment or a surface plunge point is calculated, and sediment accretion rates are reported. This formulation is developed from the mechanics of the buoyant spreading process (Akar and Jirka 1994, 1995). The definition diagram for a density current with particle settling on an incline plane in crossflow appears at the bottom of Fig. 4.

The following flux definitions along the sediment density current trajectory assume a top-hat profile distribution for velocity, suspended sediment concentration, and buoyancy:

Volume flux

$$Q = 2b_v b_h (u_c + u_a \cos \theta \cos \sigma) \quad (1)$$

Momentum flux

$$M = 2b_v b_h (u_c + u_a \cos \theta \cos \sigma)^2 \quad (2)$$

Buoyancy flux

$$J = Qg', \quad g' = \frac{\rho_a - \rho}{\rho_a} g \quad (3)$$

Clearwater volume flux

$$Q_{cw} = Q - \frac{Q_p}{\rho_{sed}} \quad (4)$$

Sediment mass flux for particle size class j

$$[Q_p]_j = 2b_v b_h (u_c + u_a \cos \theta \cos \sigma) P_j \quad (5)$$

from which the total sediment concentration is given by

$$P = \sum_j^n P_j \quad (6)$$

The change of these flux quantities along the trajectory s is given by the following conservation equations that are obtained by cross-sectional integration of the governing turbulent Reynolds equations:

Volume flux conservation accounting for turbulent entrainment

$$\frac{dQ}{ds} = E \quad (7)$$

x -momentum flux conservation (parallel to ambient flow) accounting for entrainment drag, frontal drag, bottom friction, and buoyant pressure force

$$\frac{d}{ds} (M \cos \theta \cos \sigma) = F_e + F_D \sqrt{1 - \cos^2 \theta \cos^2 \sigma} - F_\tau \cos \theta \cos \sigma - \frac{d}{ds} (F_p \cos \sigma) \quad (8)$$

Table 2. Table 2. *D-CORMIX* Simulation Output Example

X-Y-Z COORDINATE SYSTEM:
 ORIGIN is located at the SURFACE and:
 1) directly above the port center for submerged discharges, OR
 2) at the point of entry into the water for above surface discharges:
 1000.00 m from the RIGHT bank/shore.
 X-axis points downstream, Y-axis points to left, Z-axis points upward.

BEGIN MOD310: BOTTOM DENSITY CURRENT
 Profile definitions:
 BV = top-hat thickness, measured vertically
 BH = top-hat half-width, measured horizontally in Y-direction
 ZU = upper plume boundary (Z-coordinate)
 ZL = lower plume boundary (Z-coordinate)
 S = hydrodynamic average (bulk) dilution
 C = average (bulk) concentration (includes reaction effects, if any)

X	Y	Z	S	C	BV	BH	ZU	ZL
37.75	.00	-3.35	7.0	.143E+02	.97	49.19	-2.39	-3.35
50.64	.00	-3.35	10.0	.999E+01	.55	55.22	-2.80	-3.35
88.91	.00	-3.35	16.2	.619E+01	.89	85.39	-2.46	-3.35
101.66	.00	-3.35	18.5	.542E+01	.89	95.74	-2.46	-3.35
165.43	.00	-3.35	35.7	.280E+01	.89	131.90	-2.46	-3.35
216.45	.00	-3.35	390.3	.256E+00	.89	140.33	-2.46	-3.35
251.22	-65.43	-3.35	4341.0	.230E-01	115.81	181.62	112.46	-3.35
292.46	-199.42	-3.35	4538.5	.220E-01	79.35	257.25	75.99	-3.35
343.13	-316.43	-3.35	4734.9	.211E-01	66.42	313.74	63.07	-3.35
390.38	-406.77	-3.35	4910.3	.204E-01	60.55	354.61	57.20	-3.35

Cumulative travel time = 2616. sec

END OF MOD310: BOTTOM DENSITY CURRENT

PLUME SUSPENDED SEDIMENT DISTRIBUTION:

CENTERLINE (m)		DENSITY	SEDIMENT CONCENTRATIONS				(g/l or kg/m ³)	
X	Y	(kg/m ³)	SAND	C.SILT	F.SILT	CLAY	TOTAL	
.00	.00	1080.94	.00	13.00	26.00	91.00	130.00	
37.08	.00	1011.67	.00	1.68	6.12	22.28	30.08	
50.64	.00	1007.72	.00	.81	2.52	9.08	12.40	
88.91	.00	1004.48	.00	.14	1.44	5.61	7.20	
101.66	.00	1003.87	.00	.08	1.23	4.91	6.22	
165.43	.00	1001.93	.00	.01	.57	2.53	3.11	
216.45	.00	1000.17	.00	.00	.05	.23	.28	
292.46	-199.42	1000.02	.00	.00	.00	.02	.02	
343.13	-316.43	1000.01	.00	.00	.00	.02	.02	
390.38	-406.77	1000.01	.00	.00	.00	.02	.02	

CENTERLINE (m)		SEDIMENT MASS FLUXES REMAINING				(%)
X	Y	SAND	C.SILT	F.SILT	CLAY	TOTAL
37.08	.00	.00	52.69	96.06	99.86	100.00
50.64	.00	.00	62.06	97.05	99.90	95.55
63.40	.00	.00	40.80	94.53	99.81	92.85
88.91	.00	.00	17.88	89.76	99.63	89.48
101.66	.00	.00	11.84	87.47	99.55	88.36
165.43	.00	.00	1.99	78.22	99.17	85.26
216.45	.00	.00	1.07	75.21	99.04	84.47
292.46	-199.42	.00	.98	74.81	99.02	84.37
343.13	-316.43	.00	.93	74.58	99.01	84.31
390.38	-406.77	.00	.89	74.38	99.00	84.26

y-momentum flux conservation (perpendicular to ambient flow) accounting for frontal drag, bottom friction, buoyant body force, and buoyant pressure force

$$\frac{d}{ds}(M \cos \theta \sin \sigma) = -F_D \frac{\cos^2 \theta \sin \sigma \cos \sigma}{\sqrt{1 - \cos^2 \theta \cos^2 \sigma}} - F_\tau \sqrt{1 - \cos^2 \theta \cos^2 \sigma} + F_b - \frac{d}{ds}(F_p \sin \sigma) \quad (9)$$

Lateral spreading under the influence of buoyancy force against the retarding effects of frontal drag and interfacial friction (Akar and Jirka 1994, 1995)

$$\frac{db_h}{ds}$$

$$= \sqrt{\frac{-3g'b_v^2}{3C_D b_v (u_c + u_a \cos \theta \cos \sigma)^2 + 2f_i b_h (u_c + u_a \cos \theta \cos \sigma)^2}} \quad C_D = 1.0 \quad (10)$$

Clearwater buoyancy flux conservation

$$\frac{d(Q_{cw} \Delta \rho_{cw})}{ds} = Q_{cw} \frac{d\rho_a}{dx} \sqrt{1 - \cos^2 \theta \cos^2 \sigma}, \quad \Delta \rho_{cw} = \rho_a(z) - \rho_{cw} \quad (11)$$

Tracer flux conservation

$$\frac{dQ_c}{ds} = 0 \quad (12)$$

Sediment mass flux conservation accounting for particle settling

$$\frac{d[Q_p]_j}{ds} = -2b_h P_j w_j \quad \text{for particle sizes } j=1,2,3,4 \quad (13)$$

Longitudinal (x) position

$$\frac{dx}{ds} = \cos \theta \cos \sigma \quad (14)$$

Lateral (y) position

$$\frac{dy}{ds} = \cos \theta \sin \sigma \quad (15)$$

Vertical (z) position

$$\frac{dz}{ds} = \sin \theta \quad (16)$$

in which s =distance along plume trajectory; E =entrainment; θ =angle between plume centerline and horizontal plane; σ =angle between plan projection of plume centerline on the horizontal plane and the ambient current direction; F_e =entrainment force per unit length; F_D =drag force per unit length; F_p =pressure force; F_τ =bottom shear stress per unit length; F_b =body force per unit length; b_h =plume horizontal half-width; b_v =plume vertical thickness; C_D =drag coefficient (=1.0); u_a =ambient velocity; u_c =plume centerline velocity; f_i =bottom Darcy friction factor; ρ_{cw} =clearwater density; $\rho_a(z)$ =ambient density at level z ; Q_p =mass flux of sediment particles; P_j =mass density of particle size class j ; w_j =settling velocity for particle size j ; x =coordinate in downstream direction; z =vertical coordinate; and y =lateral coordinate.

The following supporting relations apply to the above equations:

Stokes settling for a particle distribution with lower size a_j and upper size b_j

$$w_j = \frac{(b_j^3 - a_j^3)}{b_j - a_j} \left[\frac{2}{27} \frac{\Delta \rho g}{\mu} \right] \quad (17)$$

Hindered settling (optional)

$$\bar{w} = w_j \left(1 - \frac{Q_p}{Q_{psed}} \right)^{4.7} \quad (18)$$

Density of sediment/water mixture

$$\rho = \rho_{cw} + P \left(1 - \frac{\rho_{cw}}{\rho_{sed}} \right) \quad (19)$$

The density current is subject to several types of entrainment mechanisms. The following entrainment definitions are adapted from surface or interface spreading density currents (Akar and Jirka 1994, 1995):

Total entrainment

$$E = E_v + E_h + E_f + E_i \quad (20)$$

Vertical entrainment from forward plume motion

$$E_v = \frac{2\alpha_v b_h u_c}{R_i^2}, \quad R_i = \frac{(\rho - \rho_a) g b_v}{\rho_a u_c^2}, \quad \alpha_v = 0.0015 \quad (21)$$

Horizontal entrainment from forward plume motion

$$E_h = 2\alpha_h b_v u_c, \quad \alpha_h = 0.057 \quad (22)$$

Frontal entrainment from perpendicular advancement of plume edge

$$E_f = \beta b_v \left[(u_a \cos \sigma + u_c) \frac{db_h}{ds} + u_a \sin \sigma \right], \quad \beta = 0.15 - 0.25 \quad (23)$$

Interfacial entrainment due to turbulence induced by bottom and interfacial shear

$$E_i = 2b_h \alpha_i \left(\left[\frac{f_b}{8} (u_c + u_a \cos \theta \cos \sigma)^2 \right]^{3/2} + \left[\frac{f_i}{8} [u_a^2 (1 - \cos^2 \theta \cos^2 \sigma)] \right]^{3/2} \right)^{1/3} \quad (24)$$

$$\alpha_i = 0.234$$

Finally, a number of internal force definitions describe the plume dynamics:

Buoyant body force/unit length

$$F_b = 2g' \sin \theta b_v b_h \quad (25)$$

Bottom shear stress/unit length

$$F_\tau = \frac{f_b}{4} b_h u_c (u_c + u_a \cos \sigma \cos \theta) \quad (26)$$

Buoyant pressure force

$$F_p = b_v^2 b_h g' \cos \theta \quad (27)$$

Drag force/unit length along plume density current front

$$F_D = C_D b_v u_a^2 (1 - \cos^2 \theta \cos^2 \sigma) \quad (28)$$

Entrainment force/unit length due to transfer of ambient momentum

$$F_e = E u_a \quad (29)$$

Laboratory Data Validation

A literature search reveals limited data for model validation of plunging density currents with sediment deposition (Alavian et al. 1992). Most laboratory experiments reported do not use sediment releases, but analyzed saline solutions to study density current behavior (Hauenstein 1982; Hauenstein and Dracos 1983; Alavian 1986; Christodoulou and Tsachou 1994). Bonnetcaze and Lister (1999) present a numerical simulation of particle driven density current down a planar slope but do not report measurement data. Only one data set presented details of a laterally unconfined density current with a suspended sediment release (Luthi 1981). This data provides the basis for an initial validation of the fundamental physical processes modeled by the *D-CORMIX*. In particular, the data can provide validation for the two fundamentally important physical processes that the model is intended to simulate: (1) the mixing, spreading, and trajectory of a density current along a sloping bottom, and (2) particle sedimentation rates.

Saline discharges permit validation of general density current trajectory and dilution, but do not allow for analysis of sedimentation effects. Several of the laboratory studies use very low velocity discharges (and, hence, low Reynolds numbers) that would not be representative for typical high velocity industrial discharge scenarios such as pipeline dredges. Discharges at low Reynolds numbers will produce laminar flow dominated by viscous forces instead of the turbulent flow typically found in large volume industrial source discharges. None of the laboratory experiments

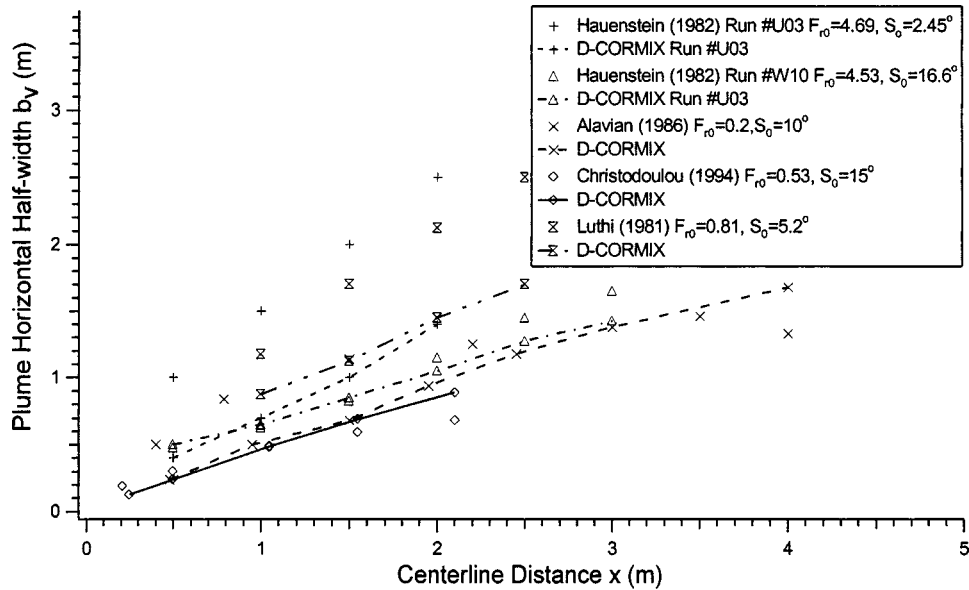


Fig. 6. Plume half-width versus centerline distance. Laboratory data set is shown by symbols, corresponding model predictions by a symbol and lines.

used for validation were conducted in the presence of an ambient crossflow. In general, the model is capable of simulating cases where $u_a > 0$, but laboratory data reflect only bottom density currents with $u_a = 0$. In addition, many of the experiments were conducted in confined laboratory tanks so that steady state conditions were often not achieved.

Fig. 6 summarizes the available laboratory data for plume lateral width (b_n) versus centerline distance. Fig. 7 shows data for plume vertical thickness (b_v) versus centerline distance. Fig. 8 shows corresponding dilution data from Hauenstein (1982). Fig. 9 shows the corresponding plume suspended sediment density and flux data and model predictions for the Luthi (1981) data set for a density current with suspended sediment. These comparisons indicate a satisfactory agreement of model predictions of density current plume dimensions and corresponding dilutions.

Using the definition of discharge Froude number

$$F_o = \frac{u_o}{\sqrt{g'_o D}} \quad (30)$$

the effect of bottom slope on plume behavior for discharges with similar Froude numbers can be seen in Fig. 6. The bottom slope and initial Froude number for Hauenstein Run No. U03 and Run No. W10 have similar Froude numbers but differing slope. A steep bottom slope causes the density current to accelerate and thus limits lateral spreading. For the shallow slope Run No. U03, *D-CORMIX* predictions appear to underpredict lateral plume spreading while width predictions for the steep slope Run No. W10 appear to be in good agreement with data.

Fig. 8 shows temperature deficit decay along the plume centerline for Hauenstein Run No. U03. In the absence of heat transfer for the short time scales in these experiments, temperature acts as a conservative tracer and its decay is directly analogous to plume dilution. *D-CORMIX* prediction of temperature decay (dilution) appears to agree very well with data. Perhaps the model underprediction of plume width and overprediction of plume depth compensate each other to produce an acceptable dilution.

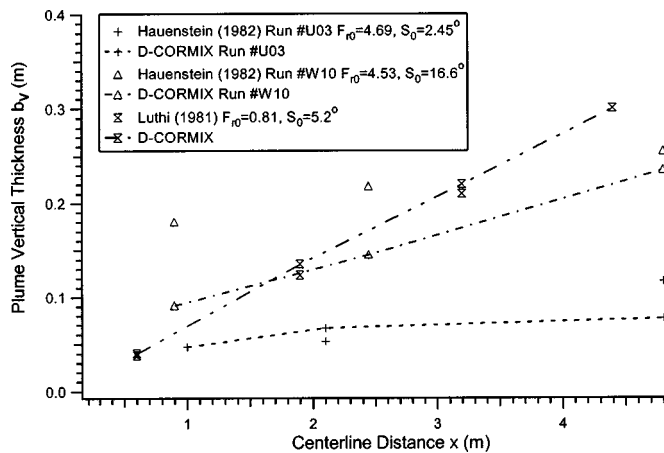


Fig. 7. Plume vertical thickness versus centerline distance for laboratory experiments

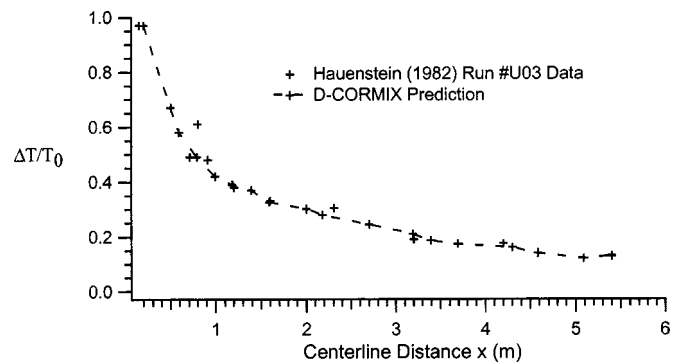


Fig. 8. Plume temperature deficit versus centerline distance. Temperature deficit is analogous to concentration.

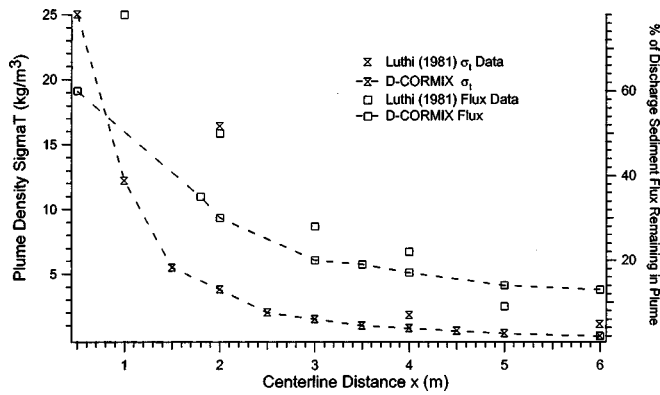


Fig. 9. Plume suspended sediment versus centerline distance

No corresponding temperature decay data was available for Run No. W10 for comparison. The Hauenstein data set appears limited in several ways: it may not be fully steady state over large distances, very limited depth (thickness) measurements are given, and no direct velocity measurements were taken.

The Luthi (1981) data set was collected in a 10 m×6 m×1 m tank. The surface source discharged 3.5 L/s for 180 s with an initial concentration of 108.4 g/L. Measurements of suspended sediment within the plume were taken with probes during the release. After the discharge stopped and all suspended plume material had settled, the tank was drained and the deposit thickness measured. The source sediment consisted of predominantly coarse silt consisting of a mean grain size of 37 μm with a standard deviation of 0.52 ϕ . Based on this description, the sediment was calculated to consist of 16% sand, 68% coarse silt, and 16% fine silt for *D-CORMIX* simulations. Details on the extent of the initial turbulent entry of the source and sediment deposition pattern were reported.

Fig. 9 compares the *D-CORMIX* predictions of suspended sediment density current dilution properties with the Luthi (1981) data. Luthi measured suspended sediment within the density current flow with a three-level suction probe, with openings located 1, 4.5, and 10 cm above the bottom, respectively, but reports only one average value for each measurement. *D-CORMIX* assumes uniform (top-hat) vertical and horizontal concentration distribution of suspended sediment within the plume. Plume density is presented in σ_t units. Assuming a sediment solids density of 2.65 kg/L, the σ_t units shown in Fig. 9 correspond to plume suspended sediment concentrations of approximately 0.5–20 g/L. Also presented in Fig. 9 is the suspended sediment flux remaining in the plume based upon calculations of the reported sediment deposit thickness. *D-CORMIX* predictions appear to be poor close to the source but improve at larger centerline distances.

Fig. 9 points to some inconsistencies that may be present in the experimental data set. Reported values of plume suspended sediment do not correspond to measured sediment deposit thickness. Plume dimensions of width and depth, given in Figs. 6 and 7, respectively, appear to be in overall good agreement with experimental results. At a centerline distance of 4 m, the data show a centerline density of 1.0017 g/cm³, which corresponds to a concentration of 7.12 g/L of suspended sediment. *D-CORMIX* predicts a density of 1.0009 g/cm³ and a suspended sediment concentration of 1.54 g/L, an underprediction by a factor of 4.6. However, the calculation of the remaining sediment flux in the plume, based on the sediment deposit thickness, would be 14% versus a predicted value of 16%. Since plume dimensions are in

Table 3. Summary of Dredge Suspended Sediment Plume Data from Mobile Bay, Ala.

Test	Sampling station number	Distance downstream x (m)	Average of all stations suspended sediment concentration c (g/L)	<i>D-CORMIX</i> prediction (g/L)
1	8	70	5.3	9.1
1	9	70	8.2	9.1
1	10	70	40	9.1
1	11	70	10	9.1
2	2	30	158	42
2	3	61	39	29
3	1	15	34	22
3	3	61	11	8.6
3	3	61	5.5	29
3	3	61	5.6	29
3	4	91	8.2	6.2
4	3	61	11	8.6
4	4	91	5.5	6.1
5	4	91	39	4.4

good agreement, the experimental plume density data would appear to be somewhat inconsistent based on conservation of mass. Perhaps the experimental plume density data is biased by the higher concentration values obtained near the bottom from the three-level probe used to sample within density current.

Field Data Validation

To assess model performance in a typical field application, the methodology was compared to data compiled from a comprehensive field study of a dredge disposal plume in Mobile Bay, Ala. (Clarke and Miller-Way 1992). This study produced extensive data on the discharge plume and benthic impacts of open water disposal. The pipeline dredge *Louisiana* was performing navigation channel maintenance in Mobile Bay with a discharge point at a local depth of 3.6 m about 330 m west of the navigation channel. The 0.635 m diameter discharge pipe was submerged 1 m below the surface with an angle of 30° to the horizontal. The discharge turbidity plume suspended sediment samples were obtained from a combination of continuous and grab samples at several downstream locations. Pipeline sediment discharge concentrations ranged from 60 to over 338 g/L, with an average of 130 g/L reported for the field study.

The study did not report sediment particle size distribution of the discharge, but available data indicate the Mobile Bay study site sediments are generally 30% silt and 70% clay (Nichols and Thompson 1978). Based on this data, the suspended sediment discharge was assumed to have a 10% coarse silt, 20% fine silt, and 70% clay particle size distribution. For all *D-CORMIX* simulations, a discharge of 2.039 m³/s containing 130 g/L of suspended sediment oriented in the direction of ambient flow, was assumed. Five tests were conducted during the study, with sampling stations located from 15 to 91 m from the discharge source, with the results shown in Table 3. To insure the data comparison accounts only for the actual suspended sediment plume, a threshold value of 1 g/L of suspended sediment was used to filter the data set to remove background noise of natural estuarine turbidity. Thus only data above 1 g/L was used to identify the plume caused

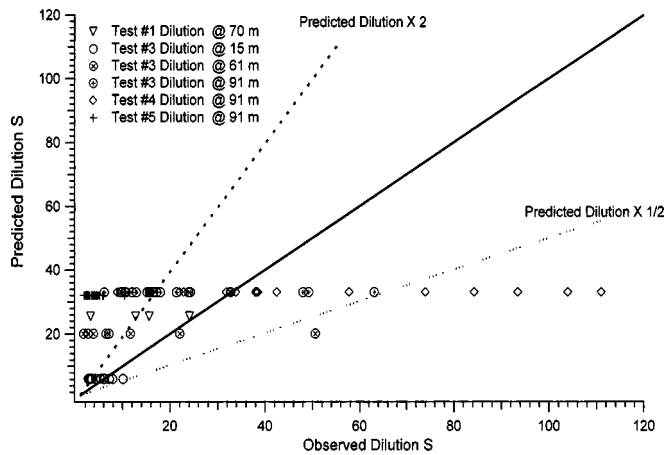


Fig. 10. Predicted versus observed sediment density current dilution S for the Alabama dredge discharge field data (Clarke and Miller-Way 1992)

by the dredge discharge. Tests No. 1 and No. 5 occurred during 0.152 m/s flood tide conditions, while test No. 2 occurred during a 0.091 m/s flood tide condition. Tests No. 3 and No. 4 occurred during 0.244 m/s ebb tides.

For tests No. 1, No. 3, and No. 4 the correlation coefficient of *D-CORMIX* predicted versus the average observed suspended sediment concentration for each station in all locations is 0.854, with *D-CORMIX* slightly underpredicting suspended sediment concentrations. Including test No. 5 (in addition to tests No. 1, No. 3, and No. 4) the correlation coefficient drops to 0.358. This is because the data indicates very high suspended sediment concentrations recorded at station 4 compared with model predictions. The correlation coefficient for all tests (tests No. 1–No. 5) is 0.918. The improvement is due to the high suspended solids concentration reported at station 2 during test No. 2 which increases the variance of the field data set. Using the following definition of dilution S

$$S = \frac{C_0}{C} \quad (31)$$

where C_0 = discharge suspended sediment concentration and C = centerline concentration of suspended sediment at a given point. Test No. 2 includes station 2 data averaging 158 g/L at 30 m downstream from the assumed discharge location, which is greater than the assumed average discharge concentration of 130 g/L. This may indicate the pipeline discharge is near the higher value of reported discharge concentration of 338 g/L rather than the assumed average discharge concentrations. Thus for test No. 2, the assumed discharge concentration of 130 g/L results in calculated dilution $S < 1$. In addition, test No. 5 indicates an average suspended solids concentration of 39,744 mg/L at station 4, at an assumed distance of 91 m from the source. This value is well above all other data values reported at this distance from the discharge. The high value may indicate that the source was located closer to the discharge than was simulated, plume material remaining from the previous tidal cycle was being reentrained during the reversal episode and reducing dilution, or a source concentration higher than the assumed 130 g/L. In summation, tests No. 1, No. 3, and No. 4 appear to be the most consistent and useful for *D-CORMIX* model validation.

The *D-CORMIX* predictions and station average data are plotted in Fig. 10. Fig. 10 shows that overall, *D-CORMIX* appears to

give reasonable, if slight underprediction, of suspended sediment concentration in dredge sediment plume density currents in a typical field application. Observed dilution varies within a given test because of the difficulties of field sampling and perhaps due to unsteady ambient and/or discharge conditions during the test. The majority of the data appear to be within a factor of 2 of the predicted values as shown by the dashed lines which appear quite satisfactory given the complexity of the phenomena and the difficulty in sampling.

In summary, the available data from laboratory and field sources show that the *D-CORMIX* density current model makes reasonable predictions of density current trajectory, dimensions, dilutions, suspended sediment concentrations, and sediment deposition mechanics.

Conclusions/Recommendations

Overall *D-CORMIX* appears to capture the essential physical processes of sediment density current plume behavior. Compared to limited laboratory data, the model presents general overall agreement with data. Most laboratory data is difficult to evaluate for model validation because of limited physical scales and poor approximation of dynamic parameters typical of industrial sediment discharges. Although *D-CORMIX* is formulated to simulate hindered settling, this option was not employed in this initial validation of the model. Researchers have reported hindered settling in plumes with concentrations greater than 10 g/L (Henry et al. 1978). Since the overall results of the laboratory data suggest that *D-CORMIX* may slightly underpredict suspended sediment concentrations especially in locations close to the discharge source where dilution is limited, additional evaluations including simulation of hindered settling in *D-CORMIX* predictions should be conducted. In addition, researchers have reported enhancement of sediment deposition due to double-diffusive convection (Garcia and Parsons 2000). This may be an important process at larger distances when the effects of hindered settling are mitigated by lower suspended sediment concentrations due to physical dilution by entrainment.

To continue the validation of the *D-CORMIX* model for sediment plume prediction, additional laboratory experiments should be conducted. Laboratory experiments are preferable to field data collection because they allow for better control of the physical processes affecting sediment density current behavior. A better understanding of the physical processes in sedimentation plumes is essential for a rigorous density current simulation model validation. The laboratory experiments should include the following features: (1) large volume sediment releases with various particle size distributions, (2) analysis of super- and subcritical transitions and discontinuities in density current behavior, (3) effects of ambient crossflow, of bottom roughness, and ambient density stratification on plume trajectory and dilution, and (4) detailed observations of spreading mechanics including measurements of vertical and lateral flow structure with plume concentrations and velocity distributions.

Acknowledgments

This study was supported through grants from USEPA Office of Water, Office of Science and Technology. Mr. Michael Kravitz, project officer, and is acknowledged for his support of this research.

Notation

The following symbols are used in this paper:

a_j = smallest radius of particle in size class j ;
 b_h = plume horizontal half-width;
 b_j = largest radius of particle in size class j ;
 b_v = plume vertical thickness;
 C_D = drag coefficient;
 c = plume centerline concentration at downstream location;
 c_0 = initial discharge concentration;
 D = discharge opening diameter;
 E = total plume entrainment;
 E_f = frontal entrainment from perpendicular advancement of plume edge;
 E_h = horizontal entrainment due to forward plume motion;
 E_i = interfacial entrainment from combined velocity sources;
 E_v = vertical entrainment due to forward plume motion;
 F = Froude number;
 F_b = body force per unit length;
 F_D = drag force per unit length;
 F_e = entrainment force per unit length;
 F_p = pressure force acting in axial direction;
 F_t = bottom shear stress per unit length;
 f_b = density current bottom Darcy friction factor;
 f_i = density current interfacial Darcy friction factor;
 f_1 = far-field Darcy friction factor;
 f_2 = near-shore Darcy friction factor;
 g = gravitational acceleration;
 g' = reduced gravitational acceleration due to density difference = $g(\rho_a - \rho_o)/\rho_a$;
 J = discharge buoyancy flux;
 M = discharge momentum flux;
 P_j = mass of particle size class j ;
 Q = total discharge volume flux;
 Q_{cw} = clear water discharge volume flux;
 Q_{pj} = flux of particle size class j ;
 Ri = flux Richardson number;
 S = dilution;
 s = centerline distance;
 s_1 = near-shore bottom slope;
 s_2 = far-field bottom slope;
 u_a = ambient velocity;
 u_c = plume centerline velocity;
 u_1 = near-shore ambient velocity;
 u_2 = far-field ambient velocity;
 v_B = lateral velocity of density current front;
 w_j = settling velocity for particle size j ;
 x = downstream coordinate;
 y = lateral coordinate;
 z = vertical coordinate;
 α_h = horizontal plume entrainment coefficient;
 α_v = vertical plume entrainment coefficient;
 β = frontal plume entrainment coefficient;
 θ_b = angle of ambient bottom slope;
 θ_0 = discharge vertical angle between port centerline and horizontal plane;
 ρ_a = ambient density at discharge level;
 ρ_{as} = ambient density at water surface;
 ρ_{a1} = ambient density at first submerged level;
 ρ_{a2} = ambient density at second submerged level;

ρ_{as} = ambient density at channel bottom;
 ρ_o = discharge density; and
 σ_0 = discharge horizontal angle, plan projection of plume centerline with the horizontal plane.

References

- Akar, P. J., and Jirka, G. H. (1991a). "CORMIX2: An expert system for hydrodynamic mixing zone analysis of conventional and toxic submerged multipoint diffuser discharges." USEPA, Athens, Ga.
- Akar, P. J., and Jirka, G. H. (1991b). "Hydrodynamic classification of submerged multipoint-diffuser discharges." *J. Hydraul. Eng.*, 117(9), 1113–1128.
- Akar, P. J., and Jirka, G. H. (1994). "Buoyant spreading processes in pollutant transport and mixing. Part 1: Lateral spreading in strong ambient current." *J. Hydraul. Res.*, 32, 815–831.
- Akar, P. J., and Jirka, G. H. (1995). "Buoyant spreading processes in pollutant transport and mixing. Part 2: Upstream spreading in weak ambient current." *J. Hydraul. Res.*, 33, 87–100.
- Akiyama, J., and Stefan, H. G. (1984). "Plunging flow into a reservoir: Theory." *J. Hydraul. Eng.*, 110(4), 484–499.
- Alavian, V. (1986). "Behavior of density currents on an incline." *J. Hydraul. Eng.*, 112(1), 27–42.
- Alavian, V., et al. (1992). "Density currents entering lakes and reservoirs." *J. Hydraul. Eng.*, 118(11), 1464–1489.
- Black, K. P., and Parry, G. D. (1999). "Entrainment, dispersal, and settlement of scallop dredge sediment plumes: Field measurements and numerical modeling." *Can. J. Fish. Aquat. Sci.*, 56, 2271–2281.
- Bonnecaze, R. T., and Lister, J. R. (1999). "Particle-driven gravity currents down planar slopes." *J. Fluid Mech.*, 390, 75–91.
- Burns, K. A., et al. (1999). "Dispersion and fate of produced formation water constituents in an Australian shelf shallow water ecosystem." *Mar. Pollution Bull.*, 38(7), 593–603.
- Chikita, K., and Okumura, Y. (1990). "Dynamics of turbidity currents measured in Katsurazawa Reservoir, Hokkaido, Japan." *J. Hydrol.*, 117, 323–338.
- Christodoulou, G., and Tsachou, F. (1994). "Experiments on 3-D turbulent density currents." *4th Annual Int. Symp. on Stratified Flows*, Grenoble, France.
- Clarke, D., and Miller-Way, T. (1992). *An environmental assessment of the effects of open water disposal of maintenance dredge material on benthic resources in Mobile Bay, Alabama*, USACOE, Vicksburg.
- Davies, P. A., et al. (1997). "Comparisons of remotely sensed observations with modeling predictions for the behaviour of wastewater plumes from coastal discharges." *Int. J. Remote Sens.*, 18(9), 1987–2019.
- Doneker, R. L., and Jirka, G. H. (1990). *CORMIX1: An expert system for mixing zone analysis of conventional and toxic single port aquatic discharges*. USEPA, Athens, Ga.
- Doneker, R. L., and Jirka, G. H. (1991). "Expert systems for mixing-zone analysis and design of pollutant discharges." *J. Water Resour. Plan. Manage.*, 117(6), 679–697.
- Doneker, R. L., and Jirka, G. H. (1997). *D-CORMIX continuous dredge disposal mixing zone water quality model laboratory and field data validation study*, Oregon Graduate Institute, Portland, Ore., 44.
- Doneker, R. L., and Jirka, G. H. (1999). "Discussion of 'Mixing in inclined dense jets,' by P. W. Roberts, A. Ferrier, and G. Daviero." *J. Hydraul. Eng.*, 125(3), 317–318.
- Ellis, D. V., et al. (1995). "Submarine tailings disposal (STD) for mines: An introduction." *Mar. Georesour. Geotechnol.*, 13, 3–18.
- Fan, J., and Morris, G. (1992). "Reservoir sedimentation: I: Delta and density current deposits." *J. Hydraul. Eng.*, 118(3), 354–369.
- Fietz, T. R., and Wood, I. R. (1967). "Three dimensional density current." *J. Hydraul. Div., Am. Soc. Civ. Eng.*, 93(6), 1–24.
- Garcia, M. (1993). "Hydraulic jumps in sediment-driven bottom currents." *J. Hydraul. Eng.*, 119(10), 1094–1117.
- Garcia, M. (1994). "Depositional turbidity currents laden with poorly sorted sediment." *J. Hydraul. Eng.*, 120(11), 1240–1263.

- Garcia, M., and Parker, G. (1991). "Experiments on hydraulic jumps in turbidity currents near a canyon-fan transition." *Science*, 245(July), 293–296.
- Garcia, M., and Parsons, J. (2000). "Enhanced sediment scavenging due to double-diffusive convection." *J. Sediment Res.*, 70(1), 47–52.
- Gawad, S. T., et al. (1996). "Near-field mixing at an outfall." *Can. J. Civ. Eng.*, 23(1).
- Hallworth, M., et al. (1998). "Effects of external flow on compositional and particle driven gravity currents." *J. Fluid Mech.*, 359, 109–142.
- Hauenstein, W. (1982). *Zuflussbedingte Dichtestromungen in Seen*, CH, ETH, Zurich.
- Hauenstein, W., and Dracos, T. (1983). "Investigation of plunging density currents generated by inflows in lakes." *J. Hydraul. Res.*, 22(3), 157–179.
- Henry, G., et al. (1978). *Laboratory investigations of the dynamics of mud flows generated by open water disposal operations*, U.S. Army, Corps of Engineers, WES, Vicksburg, Miss.
- Jirka, G. H., and Akar, P. J. (1991). "Hydrodynamic classification of submerged multiport-diffuser discharges." *J. Hydraul. Eng.*, 117(9), 1113–1128.
- Jirka, G. H., and Doneker, R. L. (1991). "Hydrodynamic classification of submerged single-port discharges." *J. Hydraul. Eng.*, 117(6), 1095–1112.
- Jirka, G. H., et al. (1996). *User's manual for CORMIX: A hydrodynamic mixing zone model and decision support system for pollutant discharges into surface waters*, DeFrees Hydraulics Laboratory, Cornell University, Ithaca, N.Y.
- Jones, G. R., et al. (1996). *CORMIX3: An expert system for mixing zone analysis and prediction of buoyant surface discharges*, DeFrees Hydraulics Laboratory, Cornell University.
- Lee, H.-Y., and Yu, W.-S. (1977). "Experimental study of reservoir turbidity current." *J. Hydraul. Eng.*, 123(6), 520–528.
- Luthi, S. (1981). "Experiments on non-channelized turbidity currents and their deposits." *Mar. Geol.*, 40, 59–68.
- McLeod, P., et al. (1999). "Behaviour of particle-laden flows into the ocean: Experimental simulation and geological implications." *Sedimentology*, 46, 523–536.
- Meinhold, A. F., et al. (1996). "Risk assessment for produced water discharges to open bays in Louisiana." *Produced water2: Environmental issues and mitigation technologies*, S. Johnson, ed., Plenum, New York.
- Mendez Diaz, M. M., and Jirka, G. H. (1996). "Buoyant plumes from multiport diffuser discharges in deep coflowing water." *J. Hydraul. Eng.*, 122(8), 428–435.
- Monaghan, J. J., et al. (1999). "Gravity currents descending a ramp in a stratified tank." *J. Fluid Mech.*, 379, 39–69.
- Mulder, T., and Alexander, J. (2001). "The physical character of subaqueous sedimentary density flows and their deposits." *Sedimentology*, 48, 269–299.
- Nash, J. D., and Jirka, G. H. (1995). *D-CORMIX continuous dredge—Cornell mixing zone expert system*, DeFrees Hydraulics Laboratory, Cornell University, Ithaca, N.Y., 6.
- Nash, J. D., and Jirka, G. H. (1996). "Buoyant surface discharges into unsteady ambient flows." *Dyn. Atmos. Oceans*, 24, 75–84.
- Neves, M. J., and Fernando, H. J. S. (1995). "Sedimentation of particles from jets discharged by ocean outfalls: A theoretical and laboratory study." *Water Sci. Technol.*, 32(2), 133–139.
- Nichols, M. M., and Thompson, G. S. (1978). *A field study of fluid mud dredged material: Its physical nature and disposal*, USACOE, Vicksburg, Miss.
- Parker, G., et al. (1986). "Self-accelerating turbidity currents." *J. Fluid Mech.*, 171, 145–181.
- Ruffin, K. K. (1998). "The persistence of anthropogenic turbidity plumes in a shallow water estuary." *Estuarine, Coastal Shelf Sci.*, 47, 579–592.
- Simpson, J. E., and Britter, R. E. (1979). "The dynamics of the head of a gravity current advancing over a horizontal surface." *J. Fluid Mech.*, 94(3), 477–495.
- Sparks, R. S. J., et al. (1993). "Sediment-laden gravity currents with reversing buoyancy." *Earth Planet. Sci. Lett.*, 114, 243–257.
- Stacey, M. W., and Bowen, A. J. (1988). "The vertical structure of density and turbidity currents: Theory and observations." *J. Geophys. Res., [Oceans]*, 93(C4), 3528–3542.
- Stow, D. A. V., and Bowen, A. J. (1980). "A physical model for the transport and sorting of fine-grained sediment by turbidity currents." *Sedimentology*, 27, 31–46.
- Tsanis, I. K., et al. (1994). "Comparison of near-field mixing models for multiport diffusers in the Great Lakes." *Can. J. Civ. Eng.*, 21(2).
- Valeo, C., et al. (1996). "Modeling Mimico Creek as a surface discharge." *J. Hydraul. Res.*, 24(1).
- Valeo, C., and Tsanis, I. K. (1996). "Two case studies of dilution models applied to thermal discharges." *Can. J. Civ. Eng.*, 23.